

Tensile testing of square structure built with electron beam melting

Bilçen Mutlu

Marmara University, Department of Mechanical Engineering, Campus 34722 Kadıköy, İstanbul

(*Corresponding author: bmutlu@marmara.edu.tr)

Submitted: 25 October 2020; Accepted: 14 June 2021; Available On-line: 17 September 2021

ABSTRACT. Nowadays, additive manufacturing (AM) makes possible the production of complex metallic parts, and the use of the titanium alloy known as Ti6Al4V with AM has become a common application through the industry. One of the most promising designs for AM is the use of lattice structures that offer light-weight parts with high strength and damping properties. Due to these features, its importance is increasing day by day in sectors requiring high technology such as aerospace. In this study, two different 2D lattice structure specimens having the same lattice density but one with wall thickness, the other one without wall thickness, have been produced with the Electron Beam Melting method and their tensile strength has experimented. Comparing the strain of both specimens, the wall thickness greatly affects the strain values. According to both FEM and tensile tests, the samples with wall thickness demonstrated improved tensile strength behavior. Production was carried out with the same production parameter values. Fracture surfaces are scanned with the Scanning Electron Microscope (SEM).

KEYWORDS: Additive manufacturing; Electron beam melting; Finite element method; Lattice structures; Scanning electron microscope; 2-D square

Citation/Citar como: Mutlu, B. (2021). "Tensile testing of square structure built with electron beam melting". *Rev. Metal.* 57(3): e200. <https://doi.org/10.3989/revmetalm.200>

RESUMEN: *Ensayo de tracción de estructuras cuadradas 2-D construidas con fusión por haz de electrones.* Hoy en día, la fabricación aditiva (AM) hace posible la producción de piezas metálicas complejas, y el uso de la aleación de titanio conocida como Ti6Al4V con AM se ha convertido en una aplicación común en la industria. Uno de los diseños más prometedores para AM es el uso de estructuras de celosía que ofrecen piezas livianas con propiedades de alta resistencia y amortiguación. Debido a estas características, su importancia está aumentando día a día en sectores que requieren alta tecnología como el aeroespacial. En este estudio, dos especímenes de estructura de celosía 2D diferentes que tienen la misma densidad de celosía, pero uno con espesor de pared, el otro sin espesor de pared, se han producido con el método de fusión por haz de electrones y se ha experimentado su resistencia a la tracción. Comparando la deformación de ambas muestras, el espesor de la pared afecta en gran medida los valores de deformación. De acuerdo con las pruebas FEM y de tracción, las muestras con espesor de pared demostraron un comportamiento mejorado de la resistencia a la tracción. La producción se llevó a cabo con los mismos valores de los parámetros de producción. Las superficies de las fracturas se escanean con el microscopio electrónico de barrido (SEM).

PALABRAS CLAVE: Cuadrado 2-D; Estructuras de celosía; Fabricación aditiva; Fusión por haz de electrones; Método de elementos finitos; Microscopio electrónico de barrido

ORCID ID: Bilçen Mutlu (<http://orcid.org/0000-0003-1598-4850>)

1. INTRODUCTION

Owing to the advancements in manufacturing methods having the ability to fabricate complex geometries, lightweight compliant structure manufacturing become increasingly desirable nowadays. Since lightweight structures can increase the product's performance, they are very in the interest of automotive and aerospace industries. An example of lightweight structures is components with an internal truss structure designed for specific loading applications. Truss structure applications were faced with some limitations in the past due to substantial cost requirements of manufacturing. However, recently, the same mechanical properties and the same exterior component design of lightweight truss structures can be obtained by additive manufacturing methods, which are cheaper than conventional manufacturing methods.

To determine the mechanical properties of the truss structures, mechanical analysis of their capabilities is necessary. And, this is the primary stage of introducing truss structures to commercial applications, which is a helpful way of choosing proper truss designs based on their weight, stiffness, and strength. Truss structures are a system of struts and nodes and for this reason they act differently from solid components under the load or weight. Finite Element Analysis (FEA) has become a standard method for component design analysis as it provides designers a fast computing system. This means designers can develop better products in a shorter time. However, the elements that FEA codes mostly used are discrete elements in the form of rods, beams, plates, or solid elements. Although all of the loading constraints such as tensile, compression, torsion, elongation, and buckling act physically on the nodes of the truss structures of different types of elements mentioned before, there exists no such truss structure having unique loading conditions all together yet. Taking into consideration such requirements, a test sample was produced in different articles with 2d lattice structure EBM (ARCAM) machine, which can be produced faster than other structures.

Electron Beam Melting (EBM) is a complete melting process through which the metal powder is fused by an electron beam with high energy (Larsson *et al.*, 2003; Shamsaei *et al.*, 2015; Galati and Iuliano, 2018). EBM is a type of Additive Manufacturing process that has the ability to produce complete density functional parts, especially complex parts made of excellent quality materials. Titanium and various titanium alloys are in the focus of this technology recently. The problem with traditional processes of titanium alloys

is their high melting point, low fluidity, and high affinity to atmospheric factors (Thompson *et al.*, 2015; Galati and Iuliano, 2018). In addition, the cost of making complex geometries by conventional manufacturing processes is very high. Vacuumed environment and high power application make the EBM method a better choice for manufacturing titanium alloys. Aerospace industry is that it is currently making full use of the benefits of manufacturing lightweight, high strength, and complex shaped material components (Gaytan *et al.*, 2009; Murr *et al.*, 2010; Biamino *et al.*, 2011). EBM process involves few manufacturing steps and in this process it is possible to recycle the powders many times without any respectable change in their physical properties and chemical composition which leads to a decrease in the overall waste material (Biamino *et al.*, 2011).

The production accomplished by using Arcam Q20 EBM machine. The machine has 2 main sections: the build chamber and the electron beam unit. The electron beam unit consists of an upper column that includes the electron generating part, and a lower column that contains the magnetic lenses. Electrons are emitted by a heated filament, the cathode, in the upper column. The potential between the anode and cathode is generally about 60 kV. Magnetic lenses control the shape and the deflection of the electron beam (Galati and Iuliano, 2018; Del Guercio *et al.*, 2020). The shape of the beam is corrected by the first set of coils (astigmatic lenses). The second set of coils (focus lenses) are responsible for controlling the size of the beam (Gong *et al.*, 2012; Galati and Iuliano, 2018).

The function of the last set of coils (deflection lenses) is to position the beam on the built platform according to a sliced geometry (Froes and Dutta, 2014). To avoid air molecules from diffusing the EBM, the whole process occurs in a vacuum that is created using turbo-molecular pumps. The pressure inside the processing chamber is generally at around 10-4 mPa (Biamino *et al.*, 2011). To ensure the thermal stability of the process and to prevent the formation of electrical charges in the powder, a small amount of inert helium gas is added during the melting process (Gaytan *et al.*, 2009). After finishing the process, the helium pressure is raised to ease cooling (Gaytan *et al.*, 2009). Three main components of the build chamber are: the powder feeder, the raking system, and the steel build tank. The steel build tank, which can be moved along the Z-axis, contains the process platform that constitutes the X-Y build plane. Before starting the process, the process platform, the start plate, is heated. There are two hoppers, which are located in the upper left and right corners of the built chamber. These hoppers are the

components of the powder storing system. The powder material of Arcam is typically produced by the gas atomization method or through a plasma rotating electrode process (Gu, 2015). The spherical shaped particles have the common size of 45-100 μm . Powders that are collected by the rake from the sides move over the surface and as a result they form a uniformly distributed layer over the X-Y built plane. Uniformity in thickness is important in terms of lack of fusion and pushing phenomenon.

2. MATERIALS AND METHODS

2.1. Ti-6Al-4V material properties

In additive manufacturing technologies, there are many melting technologies. In this study, the tensile specimen is manufactured with electron beam melting. The width of the α -laths affects the tensile strength of EBM samples. As α -lath gets coarser, the tensile strength of the sample decreases. In other words, a slight increase in the temperature of the building chamber causes a drastically reduction in the tensile strength. Yield strength and hardness of many materials depend on the grain size. Some mechanical properties of Ti-6Al-4V alloy change with the size of the prior β -grains. According to Hall-Petch relation:

$$\sigma_y = \sigma_0 + \frac{K}{\sqrt{D}}$$

where σ_0 is the single crystal yield strength, K is a material constant, and D the grain diameter, the yield strength (σ_y) decreases as the grain size increases. Coverage and dislocation density are other factors affecting the yield strength of materials (Rafi *et al.*, 2013; Simonelli *et al.*, 2014a; Leicht and Wennberg, 2015).

There are two types of pores in AM components: long and spherical. Long pores can form as a result of incorrect melting of the built layers, and spherical ones occur due to the presence of argon gas in the dust (Simonelli *et al.*, 2014b). Pores have various effects on mechanical properties depending on the building direction. Porosity between layers reduces the yield strength and UTS of samples filtered perpendicular to the sheet direction (Simonelli *et al.*, 2014b). However, the pores have a limited effect on layer-oriented samples parallel to the stretching direction because they contain fewer layers and have a lower chance of forming pores. According to the manufacturer

of our EBM machine, Arcam, the materials delivered must have mechanical properties as shown in Table 1.

2.2. Specimen preparation

2.2.1. Modeling parameters of specimens

Many different lattice structure models are used in additive manufacturing. 2-D square lattice structure is the simplest, which is selected for this study.

There are numerous reasons for utilizing the unit cell design approach. It causes faster FEA calculation by decreasing the computational intensity of the calculations via introducing the unit cell as an element type in a Finite Element Analysis as opposed to the prevalent FEA method of defining many nodes and struts containing the truss structure. This approach also has another advantage which is the ability of using less dense unit cells in locations that are carrying less load which leads to a maximum component performance (Arabnejad and Pasini, 2013). In the FEA model of the wall thickness and without wall thickness samples, the regions where the break will occur are modeled as mid surface. These regions are meshed with a smaller density. Number of elements in these regions, it is defined as approximately 1.300.000 million. The analyzes were carried out as explicit dynamics. It can be seen in Figs. 5-6 that the fractures that occur in FEA occur in the regions close to the test results.

Tensile samples were produced according to ASTM E8 standards. The tensile test specimen created for the ASTM E8M-04 (2004) standard is shown in Fig. 1. Each specimen was built with the same process parameters. Process parameters for melting stage are shown in Table 2.

In this study, SpaceClaim is used for model the specimens which were used in tensile testing. Specimen details are shown below in Fig. 2. The details about the specimen's dimensions are given Table 3. Leicht and Wennberg made tensile tests on three samples. According to their test data, the vertical orientation of production is usually better in terms of tensile strength (Leicht and Wennberg, 2015).

The reason is related to the microstructure and especially the direction of growth of the previous grains. While β grains grow along the stretching direction in all samples built in the Z direction, the grain growth of the previous β beads is per-

TABLE 1. Key mechanical properties of EBM produced components

Yield Strength (MPa)	UTS (MPa)	Elongation to fracture (%)
950	1020	14

TABLE 2. EBM process melting stage parameters

Beam Speed	Beam Current	Beam Offset	Beam Current	Line Offset	Surface Temperature
400-450 mm·s ⁻¹	7 mA	0.18-0.27 mm	35 mA	0.22 mm	925 °C

TABLE 3. Tensile Specimen's parameters

Density	Length of unit lattice structure	Thickness of unit lattice structure	Wall Thickness (Specimen-2)	Direction of printing
65.8%	1.69 mm	1.2 mm	1 mm	Z-direction

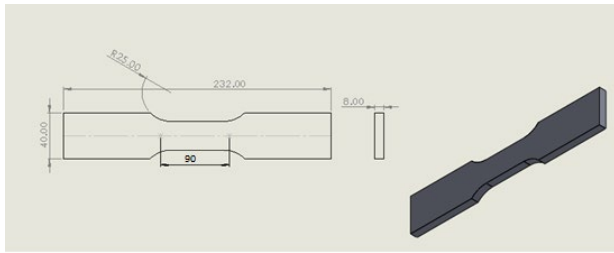


FIGURE 1. Dimensions of tensile test specimen according to ASTM E8M.

pendicular to the drawing direction in all samples built in the X direction, as shown in Fig. 3. The anisotropic behavior of the previous β grains reveals greater crack deflection ability in Z-directional samples (Leicht and Wennberg, 2015; Mezzetta *et al.*, 2018).

Tensile tests were made with Instron 8802 hydraulic test machine by ASTM D3039M-17 (2017) Width and thickness values of specimens entered to the system with the test speed of 0.5 mm·min⁻¹.

2.2.2. Mesh processing and FEA analysis

For this analysis, plasticity was defined as the material by using Bilinear Isotropic Hardening Behavior. In general, material nonlinearities occur because of the nonlinear relationship between stress and strain. This relationship is, except for the case of nonlinear elasticity and hyperelasticity, path-dependent, thus the stress depends on the strain history as well as the strain itself (Dinita *et al.*, 2018). Bilinear isotropic hardening is recommended for large strain analysis (ANSYS, 2009). Lattice Structures have very small and detailed surfaces, so it can be hard to mesh them. In this study, lattice structures are modelled as shell elements (2-D Body) by using SpaceClaim's midsurface command. As shown in Fig. 4, 21276 nodes and 18876 first-order hex elements were used. Mesh is done in different iterations. Analyzes were continued until the mesh converged. The analysis results could not converge to the test results due to the insufficient processor of the computer where the analyzes were made. The last iteration was carried out with 1.350.000 nodes,

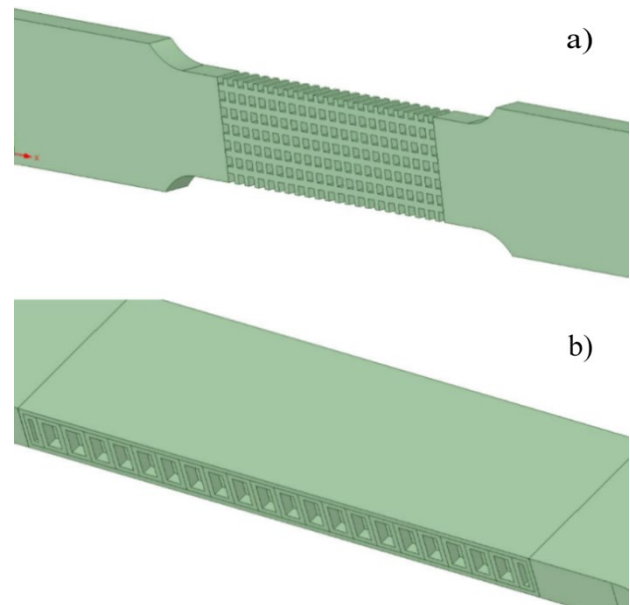


FIGURE 2. View of (a) Specimen-1 and (b) Specimen-2 in X-Y-Z Plane (with wall).

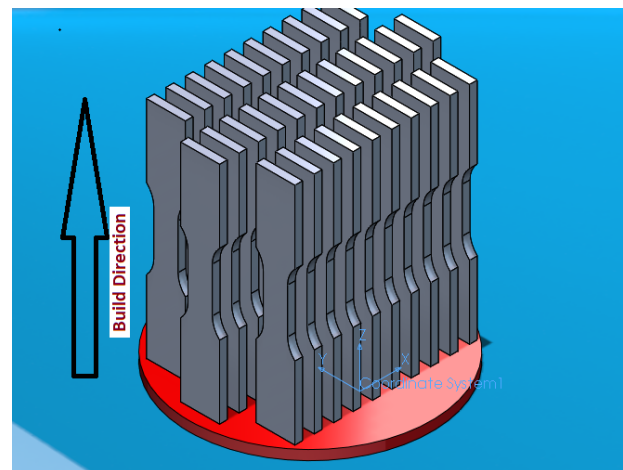


FIGURE 3. Build Direction along Z-axis.

1.134.00 elements. Figures 5-6 shows that the results of the FEA analysis of the sample with and without the wall thickness are shown. In the analysis, the boundary condition was given as in the tensile test machine. That is, one end of the tensile

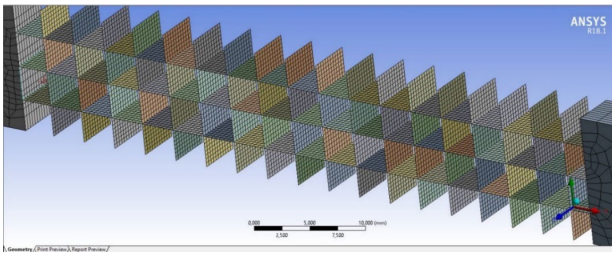


FIGURE 4. Lattice Structures Meshing.

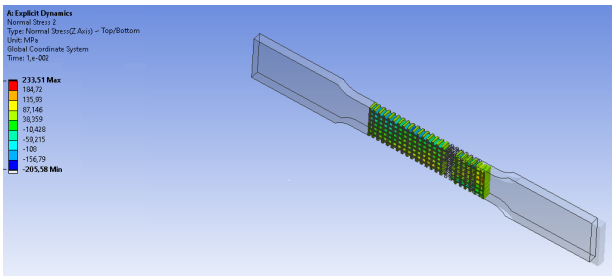


FIGURE 5. Sample without wall thickness FEA results.

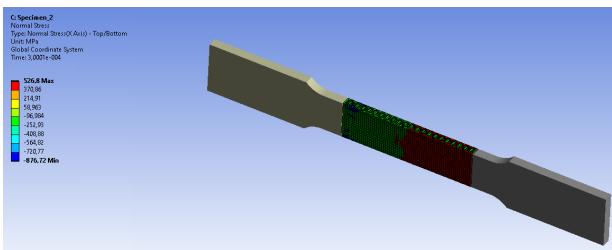


FIGURE 6. Sample wall thickness FEA results.

sample is fixed and the other end is loaded with a time-dependent load.

3. RESULTS

In a cellular model, the characteristic length of the unit cell is generally considered several times less than the characteristic length of the component. Unit cell study is necessary in terms of understanding the mechanical response of the material at the macroscale. Several analytical and numerical approaches have been proposed in the literature, along with some experimental research to determine the mechanical properties of cellular models (Guedes and Kikuchi, 1990; Chen and Huang, 1998). The most important studies in this field are Gibson and Ashby (1999), Masters and Evans (1996), Christensen (2000), and Wang and McDowell (2004). In all of these works, the cell walls are assumed to behave like Euler–Bernoulli beams. Moreover, the examination of individual cell walls and determination of the cell elastic constants are the subjects of these studies. According to the information given above, it was discussed that lower mechanical properties were obtained compared to

the mechanical properties of the titanium material produced in the work. The production of both wall thickness and non-wall thickness samples are produced with the same density values. The reason is to compare the tensile test and analysis results clearly.

Tensile tests for samples with and without wall thickness were performed. For the test samples with and without wall thickness, a total of 12 samples, 6 in each group, were produced. In the study, the tensile test results of only the best performed specimens from both groups are given and the other specimen results are shown in standard deviation diagram. The samples without wall thickness are shown in Fig. 7. Since the results of the tensile test of the sample can be seen from Fig. 9, the strain and tensile strength values are quite low. Therefore, these samples cannot work under most of the tensile load applications. The samples are shown in Fig. 8, which

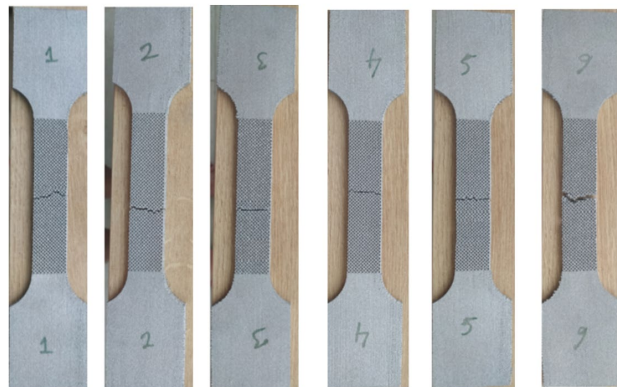


FIGURE 7. Images of specimens without wall.

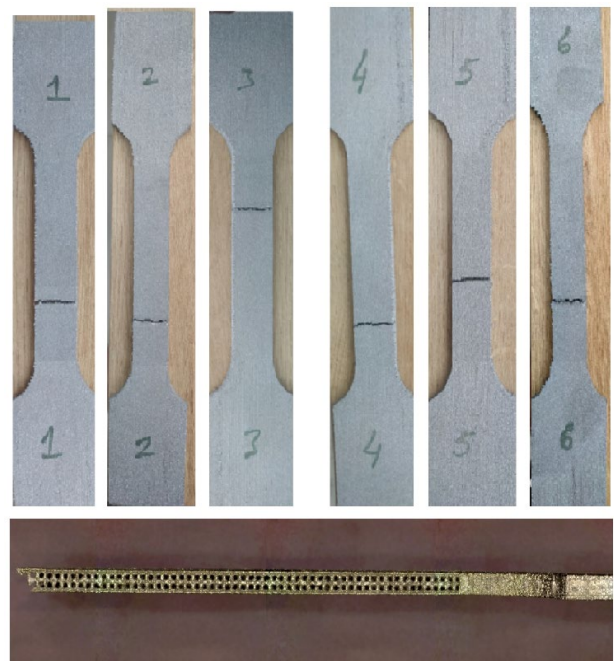


FIGURE 8. Images of the specimens with wall.

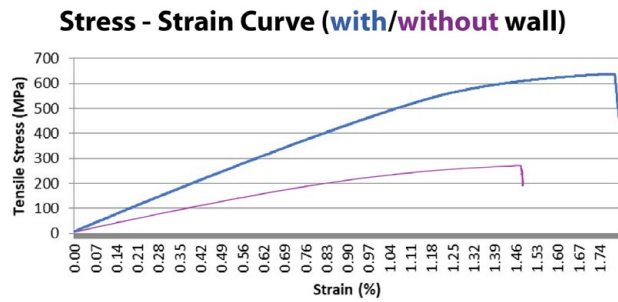


FIGURE 9. Stress-Strain curve of specimen with/without wall.

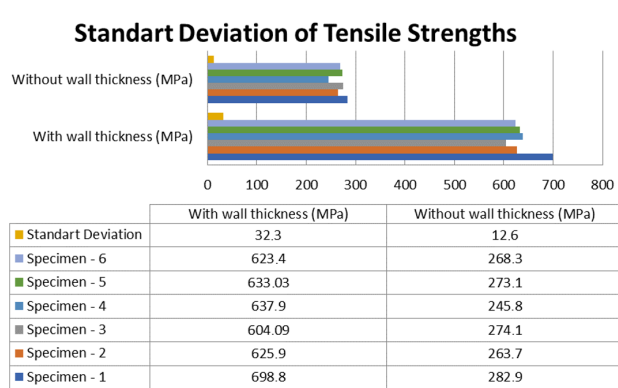


Figure 10. Standard deviation of tensile samples.

includes a wall thickness, are performed better under tensile load. The Stress-Strain curve in Fig. 9 proves that it also has high elongation values. Therefore, it can be used in mechanical components operating under tensile load.

Each result of both analysis and tensile test were compared, the results of both samples were slightly different. The reason of this difference can be observed from SEM images. Finite element analysis and tensile test results are shown in Table 4.

As can be seen from Fig. 10, 6 samples from each group were tested. The standard deviation of each group of tested samples is also shown. The specimens named as Specimen – 1 are the specimens which are mainly investigated above.

4. DISCUSSION

In their research, Shunmugavela et al. compared the microstructure and mechanical properties of Ti6Al4V produced by forging and EBM. They examined the fracture surfaces using an electron microscope (SEM) and found that there were a large number of small size pits on the surface of the parts produced with EBM, causing breakage. The forged

titanium profile showed deep pits which is a ductile behavior of the material (Shunmugavel *et al.*, 2015). Quénard et al. examined the tensile fracture surfaces of Ti6Al4V produced as an additive and showed that the failure mechanism was mostly ductile. They also observed microcracks with brittle surfaces around them. They connected these fragile surfaces to split in layers where the two ductile surfaces were joined, and concluded that the ductility of the samples was dominant, although they showed a mixed ductile brittle behavior (Quénard *et al.*, 2018).

In this study, the fracture characteristics of the samples were close to the ones examined by others which mentioned above. Tensile samples showed the characteristics of ductile brittle fracture as can be seen in Figs. 11-12. Figure 11 shows the dimple on the walls of the wall thickness sample, these deep pits cause the sample to break prematurely in the tensile test. Figure 12 represents the fracture area

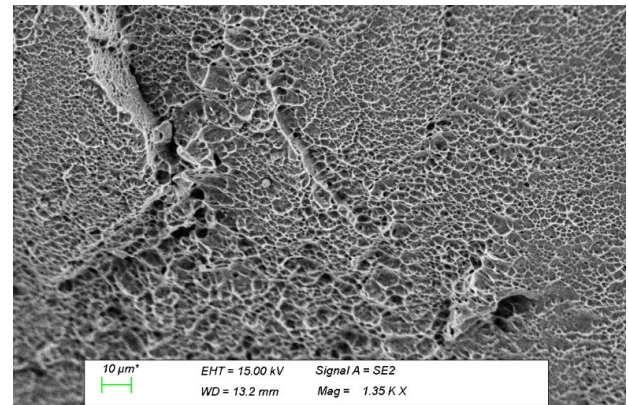


Figure 11. Images of fracture surface on wall structure.

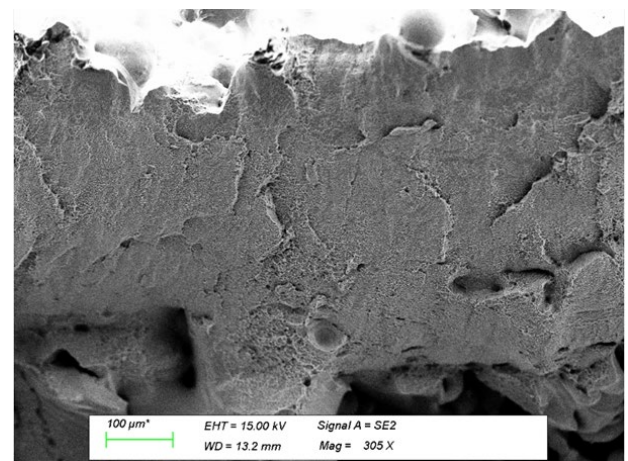


Figure 12. Fracture surface on lattice structure.

TABLE 4. Comparison of data from tensile test and analysis

Specimen Type	FEM Stress (MPa)	Tensile Test Stress (MPa)
With Wall	526.8	698.8
Without Wall	233.5	282.9

of the samples and it points out that the fracture is brittle.

A fracture that spreads through crystallographic low index planes is the low energy fracture (Dietter, 1986). This break is accompanied with cleavage facets that are flat. When the crack propagates on a number of planes of varying elevations, the river's markings separate the facets (Erdogan and Tekeli, 2002). The transgranular ductile dimple tearing on the fracture surface of the EBM-produced Ti6AL4V sample results from the coalescence of microvoids. The extent of plastic deformation is indicated by a healthy population of fine bolts on the tensile fracture surface (Rafi *et al.*, 2013).

Figure 13 shows the fracture surfaces of the samples (2-5) with wall thickness in one direction. It is observed that the piece breaks brittle from the frac-

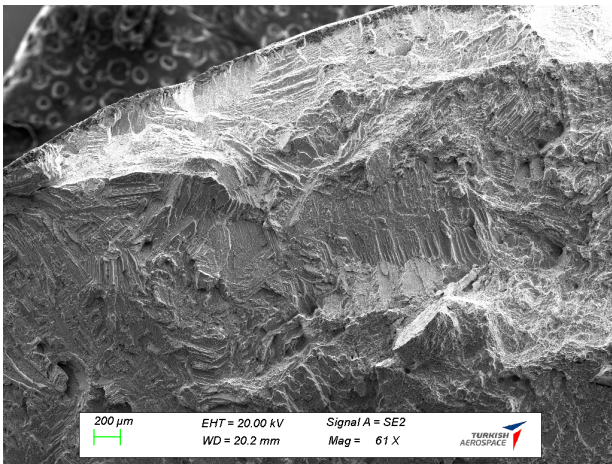


Figure 13. Fracture surface 2-3th sample with wall thickness.

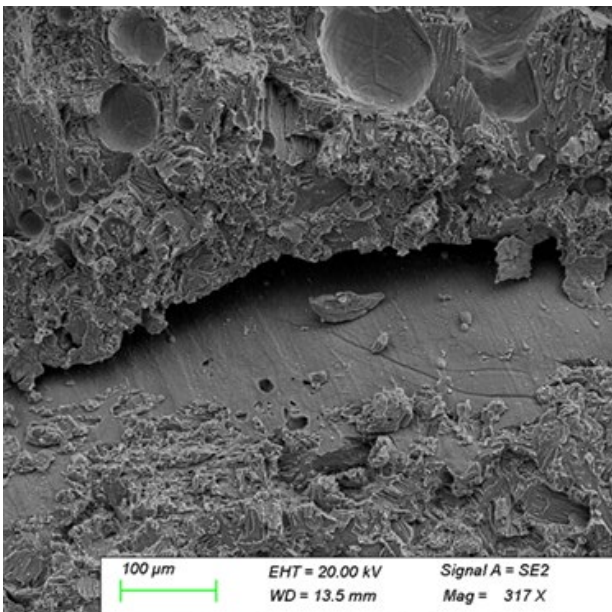


Figure 14. 3-5th specimen fracture surface without wall thickness.

ture surfaces. When we compare it with other wall thickness samples, we can see that the fractures are brittle in a particular sample. When we look at a lattice structure of the sample with wall thickness in Fig. 14, it was observed that the fracture occurred from these vertical lattice structures. Residual stresses and metal voids in the part are the main causes of fracture. Since the images of all tensile specimens with and without wall thickness are very close to each other, it was deemed appropriate to share two SEM images from each group.

5. CONCLUSIONS

- 2-D Square Lattice Structures with and without wall thickness were analyzed for unit cells consisting of the same density structures. Test samples were produced and tensile tests were performed. A comparison was made between FEA and test results for both groups of specimens. Due to boundary conditions, the nonlinearization approach, mesh and elemental quality caused the difference between analysis and test results.
- Early studies showed that process parameters are the most important criteria for the tensile strength results. As the EBM process melts the metal powders, there is a possibility that some powders will not melt properly and the bonds will be weak on those areas. Lots of experiments have been made to acquire the proper parameters for this design and the best results are investigated in this study. When looking at the SEM results of the test samples, ductile-brittle fracture behavior was observed. The same situation can be seen in the stress-strain curve. From the tensile test, it was observed that the structure with wall thickness has higher strength than the structure without wall thickness. It is also clear that the wall-thickness structure has more elongation.
- According to the test and analysis results, wall addition to the lattice structures is more applicable for regions working under tensile loads.
- The nonmelting metal powders on the surface of the parts produced with EBM significantly change the mechanical properties of the part. Because of this reason, the produced samples must be subjected to secondary processings such as machining, heat treatment, hot isostatic pressing etc. Considering the effect of wall thickness on tensile strength, the importance of the design stage shows itself. This study also proves that the production of geometry which includes thin structures such as lattices requires careful preparation.

ACKNOWLEDGEMENTS

In the study, all of the specimens subjected to the tensile test were produced in the Turkish

aviation (TUSAS) industry. In addition, each of the tests was carried out in TUSAS facilities. We would like to thank you for the opportunities provided by the Turkish aviation industry.

REFERENCES

- ANSYS (2009). Structural Analysis Guide. Release 12.1, USA, SAS IP, Inc.
- ASTM E8M-04 (2004). Standard Test Methods for Tension Testing of Metallic Materials. ASTM International, West Conshohocken, PA.
- ASTM D3039M-17 (2017). Standard Test Method for Tensile Properties of Polymer Matrix Composite Materials. ASTM International, West Conshohocken, PA.
- Arabnejad, S., Pasini, D. (2013). Mechanical properties of lattice materials via asymptotic homogenization and comparison with alternative homogenization methods. *Int. J. Mech. Sci.* 77, 249–262. <https://doi.org/10.1016/j.ijmecsci.2013.10.003>.
- Biamino, S., Penna, A., Ackelid, U., Sabbadini, S., Tassa, O., Fino, P., Pavese, M., Gennaro, P., Badini, C. (2011). Electron beam melting of Ti-48Al-2Cr-2Nb alloy: Microstructure and mechanical properties investigation. *Intermetallics* 19 (6), 776–781. <https://doi.org/10.1016/j.intermet.2010.11.017>.
- Chen, J.Y., Huang, M., Ortiz, M. (1998). Fracture analysis of cellular materials: A strain gradient model. *J. Mech. Phys. Solids*. 46 (5), 789–828. [https://doi.org/10.1016/S0022-5096\(98\)00006-4](https://doi.org/10.1016/S0022-5096(98)00006-4).
- Christensen, R.M. (2000). Mechanics of cellular and other low-density materials. *Int. J. Solids Struct.* 37 (1-2), 93–104. [https://doi.org/10.1016/S0020-7683\(99\)00080-3](https://doi.org/10.1016/S0020-7683(99)00080-3).
- Del Guercio, G., Galati, M., Saboori, A., Fino, P., Iuliano, L. (2020). Microstructure and Mechanical Performance of Ti-6Al-4V Lattice Structures Manufactured via Electron Beam Melting (EBM): A Review. *Acta Metall. Sin. (Engl. Lett.)* 33, 183–203. <https://doi.org/10.1007/s40195-020-00998-1>.
- Dieter, G.E. (1986). *Mechanical Metallurgy*. McGraw Hill, New York.
- Dinita, A., Lambrescu, I., Chebakov, M.I., Dumitru, G. (2018). *Finite Element Stress Analysis of Pipelines with Advanced Composite Repair*. In: Barkanov E., Dumitrescu A., Parinov I. (eds) *Non-destructive Testing and Repair of Pipelines*. Springer, Cham. pp. 289–309. https://doi.org/10.1007/978-3-319-56579-8_18.
- Erdogan, M., Tekeli, S. (2002). The Effect of Martensitic Particle Size on Tensile Fracture of Surface-Carburized AISI, 8620 Steel with Dual Phase Core Microstructure. *Mater. Design* 23 (7), 597–604. [https://doi.org/10.1016/S0261-3069\(02\)00065-1](https://doi.org/10.1016/S0261-3069(02)00065-1).
- Froes, F.H., Dutta, B. (2014). The additive manufacturing (AM) of titanium alloys. *Adv. Mat. Res. Trans. Tech. Publ.* 1019, 19–25. <https://doi.org/10.4028/www.scientific.net/AMR.1019.19>.
- Galati, M., Iuliano L. (2018). A literature review of powder-based electron beam melting focusing on numerical simulations. *Addit. Manuf.* 19, 1–20. <https://doi.org/10.1016/j.addma.2017.11.001>.
- Gaytan, S.M., Murr, L.E., Medina, F., Martinez, E., Lopez, M.I., Wicker, R.B. (2009). Advanced metal powder based manufacturing of complex components by electron beam melting. *Mater. Technol.* 24 (3), 180–190. <https://doi.org/10.1179/106678509X12475882446133>.
- Gibson, L.J., Ashby, M.F. (1999). *Cellular Solids: Structure and Properties*. Cambridge University Press.
- Gong, X., Anderson, T., Chou, K. (2012). Review on powder-based electron beam additive manufacturing technology. IFA 2012, Proceedings of the ASME, pp. 507–515. <https://doi.org/10.1051/mfreview/2014001>.
- Gu, D. (2015). *Laser Additive Manufacturing of High-performance Materials*. Springer.
- Guedes, J., Kikuchi, N. (1990). Preprocessing and postprocessing for materials based on the homogenization method with adaptive finite element methods. *Comput. Methods Appl. Mech. Eng.* 83 (2), 143–198. [https://doi.org/10.1016/0045-7825\(90\)90148-F](https://doi.org/10.1016/0045-7825(90)90148-F).
- Larsson, M., Lindhe, U., Harrysson, O. (2003). Rapid Manufacturing with Electron Beam Melting (EBM) – A manufacturing revolution?. Inter. Solid Freeform Fabrication Symposium, pp. 438–443. <http://dx.doi.org/10.26153/tsw/5603>
- Leicht, A., Wennberg, E.O. (2015). Analyzing the Mechanical Behavior of Additive Manufactured Ti-6Al-4V Using Digital Image Correlation. Diploma work in the Master programme Materials Engineering, Chalmers University of Technology, Gothenburg, Sweden.
- Masters, I., Evans, K. (1996). Models for the elastic deformation of honeycombs. *Compos. Struct.* 35 (4), 403–22. [https://doi.org/10.1016/S0263-8223\(96\)00054-2](https://doi.org/10.1016/S0263-8223(96)00054-2).
- Mezzetta, J., Choi, J.P., Milligan, J., Danovitch, J., Chekir, N., Bois-Brochu, A., Zhao, Y.F., Brochu, M. (2018). Microstructure-Properties Relationships of Ti-6Al-4V Parts Fabricated by Selective Laser Melting. *Int. J. Precis. Eng. and Manuf.-Green Tech.* 5, 605–612. <https://doi.org/10.1007/s40684-018-0062-1>.
- Murr, L.E., Gaytan, S.M., Medina, F., Martinez, E., Martinez, J.L., Hernandez, D.H., Machado, B.I., Ramirez, D.A., Wicker, R.B. (2010). Characterization of Ti-6Al-4V open cellular foams fabricated by additive manufacturing using electron beam melting. *Mater. Sci. Eng. A* 527 (7-8), 1861–1868. <https://doi.org/10.1016/j.msea.2009.11.015>.
- Quénard, O., Dorival, O., Guy, Ph., Voté, A., Brethome, K. (2018). Measurement of fracture toughness of metallic materials produced by additive manufacturing. *CEAS Space J.* 10 (3), 343–353. <https://doi.org/10.1007/s12567-018-0202-z>.
- Rafi, H.K., Karthik, N.V., Gong, H., Starr, T.L., Stucker, B.E. (2013). Microstructures and Mechanical Properties of Ti6Al4V Parts Fabricated by Selective Laser Melting and Electron Beam Melting. *J. Mater. Eng. Perform.* 22 (12), 3872–3883. <https://doi.org/10.1007/s11665-013-0658-0>.
- Shamsaei, N., Yadollahi, A., Bian, L., Thompson, S.M. (2015). An overview of Direct Laser Deposition for additive manufacturing; Part II: Mechanical behavior, process parameter optimization and control. *Addit. Manuf.* 8, 12–35. <https://doi.org/10.1016/j.addma.2015.07.002>.
- Shunmugavel, M., Polishetty, A., Littlefair, G. (2015). Microstructure and mechanical properties of wrought and Additive manufactured Ti-6Al-4V cylindrical bars. *Procedia Technol.* 20, 231–236. <https://doi.org/10.1016/j.protec.2015.07.037>.
- Simonelli, M., Tse, Y.Y., Tuck, C. (2014a). The formation of $\alpha + \beta$ microstructure in as-fabricated selective laser melting of Ti-6Al-4V. *J. Mater. Res.* 29, 2028–2035. <https://doi.org/10.1557/jmr.2014.166>.
- Simonelli, M., Tse, Y.Y., Tuck, C. (2014b). Effect of the building orientation on the mechanical properties and fracture modes of SLM Ti-6Al-4V. *Mater. Sci. Eng. A* 616, 1–11. <https://doi.org/10.1016/J.MSEA.2014.07.086>.
- Thompson, S.M., Bian, L., Shamsaei, N., Yadollahi, A. (2015). An overview of Direct Laser Deposition for additive manufacturing; Part I: Transport phenomena, modeling and diagnostics. *Addit. Manuf.* 8, 36–62. <https://doi.org/10.1016/j.addma.2015.07.001>.
- Wang, A., McDowell, D. (2004). In-plane stiffness and yield strength of periodic metal honeycombs. *J. Eng. Mater. Technol.* 126 (2), 137–156. <https://doi.org/10.1115/1.1646165>.